A time domain fast boundary integral equation method for three dimensional elastodynamics

理化学研究所　高橋 徹 (Toru Takahashi)　　京大・工学研究科　西村 直志 (Naoshi Nishimura)
The Institute of Physical and Chemical Research　　Department of Civil Engineering, Kyoto Univ.

1　Introduction

Boundary Integral Equation Method (BIEM) is considered to be an efficient solver for exterior problems. This is particularly true in wave problems such as those in acoustics, electromagnetics and elastodynamics, because there is no need to introduce techniques to avoid non-physical reflections from artificial boundaries with BIEM. Indeed, one can find examples of successful use of BIEM in wave related engineering problems in literature (See Kobayashi et al. [1] for example). It is therefore considered to be worth the efforts to further enhance the performance of BIEM in wave problems by investigating a fast method.

In elastodynamics, one can find some attempts to develop fast BIEM in frequency domain, as reviewed in Nishimura [2]. In time domain, however, not much has been done except in the work by Takahashi et al. [3] where these authors extended the approach by Lu et al. [4] in the wave equation to elastodynamics in 2D. As a matter of fact, one may say that almost all of the fundamentals of the fast BIEM in wave problems in time domain have so far been developed in Michielssen's group. Their most advanced approach is found in Ergin et al.[5] where they proposed a fast method (Plane Wave Time Domain (PWTD) algorithm) for the wave equation in 3D which utilises the plane wave expansion of the fundamental solution in the space-time and a multilevel implementation. See Nishimura [2] for more references.

The purpose of this paper is to continue the efforts by Takahashi et al. [3] in 2D, and to extend the PWTD approach to elastodynamics in 3D. As we shall see the extension is straightforward, but is by no means automatic. This is because of the presence of two waves (P and S waves) in elastodynamics and the time integration found in the elastodynamic fundamental solution. In view of this, we shall present the detail of the derivation of the plane wave expansion for elastodynamics in this paper.

This paper begins with the fundamentals of the BIEM in the time domain elastodynamics in 3D. After a brief recapitulation of the time-marching method with the conventional BIEM, we derive the plane wave expansion of the time domain elastodynamic fundamental solution in 3D in section 2. After preparing some mathematical tools, we proceed to the description of the algorithm in section 3. It is shown that the complexity of the proposed approach is either $O(N_s \log^2 N_s N_t)$ or $O(N_s^{3/2} N_t)$ depending on the algorithm used for the Legendre transformation. The performance of the proposed algorithm is tested in section 4 where problems having the spatial DOF of $O(10^4)$ are considered. The proposed approach is concluded to outperform the conventional BIEM even in the smallest problem considered.

2　Formulation

2.1　Governing equations and BIE

Let $D \subset \mathbb{R}^3$ be a domain having a smooth boundary $\partial D = S$. The initial boundary value problem for 3 dimensional elastodynamics in time domain is formulated as follows: To solve

$$\mu u_{i,jj}(x,t) + (\lambda + \mu)u_{j,ij}(x,t) + b_i(x,t) = \rho \ddot{u}_i(x,t) \tag{1}$$

for the unknown vector function (displacements) $u_i(x,t)$ ($x = (x_1, x_2, x_3) \in D, t \in (0, \infty)$) subject to certain initial and boundary conditions, where u stands for the displacement vector, x and t are the spatial variable and time, λ and μ are Lamé's constants, ρ is the density and b is the body force per unit volume, respectively. Also, we have used the summation convention for repeated indices. As typical initial and boundary conditions we consider the following:

$$
\begin{aligned}
\text{initial condition} \quad & u(x,0) = \dot{u}(x,0) = 0 \quad \text{in } D \\
\text{boundary condition} \quad & u(x,t) = \bar{u}(x,t) \quad \text{on } S_1 \\
& t(x,t) = \bar{t}(x,t) \quad \text{on } S_2
\end{aligned}
\tag{2}
$$

where $(\bar{\cdot})$ indicates a function given on the boundary. Also, S_1 and S_2 are parts of the boundary S such that $S = S_1 + S_2$ holds, and t stands for the traction defined by

$$t_i(x,t) = C_{ijkl} n_j(x) u_{k,l}(x,t),$$

where n is the outward normal vector to S and C_{ijkl} is the elasticity tensor defined in terms of Lamé's constants λ and μ by $C_{ijkl} = \lambda \delta_{ij}\delta_{kl} + \mu(\delta_{ik}\delta_{jl} + \delta_{il}\delta_{jk})$.

Assuming the body force to vanish, we obtain from (1) the following boundary integral equation:

$$\frac{1}{2}u_i(x,t) + \int_S T_{ij}(x,y,t) * u_j(y,t)dS_y = \int_S \Gamma_{ij}(x-y,t) * t_j(y,t)dS_y \quad x \in S, \quad t > 0 \tag{3}$$

where the superimposed $-$ stands for the Cauchy principal value of an integral and $*$ indicates the convolution with respect to time. The integrals on the RHS and LHS of (3) are called the single and double layer potentials, respectively, whose kernels Γ and T are defined by

$$\Gamma_{ij}(x,t) = \frac{1}{4\pi\mu}\left[\frac{\delta(t-|x|/c_T)}{|x|}\delta_{ij} - c_T^2\partial_i\partial_j\left(\frac{(t-|x|/c_T)_+}{|x|} - \frac{(t-|x|/c_L)_+}{|x|}\right)\right], \tag{4}$$

$$T_{ij}(x,y,t) = C_{jlnm}n_l(y)\frac{\partial}{\partial y_n}\Gamma_{im}(x-y,t) \tag{5}$$

where c_L and c_T are velocities of P and S waves defined by

$$c_L = \sqrt{\frac{\lambda+2\mu}{\rho}}, \quad c_T = \sqrt{\frac{\mu}{\rho}},$$

δ_{ij} is Kronecker's delta and $f_+ = (|f| + f)/2$.

2.2 Plane wave expansions of the kernels

The most important ingredient in the proposed fast method of solving integral equations in time domain is the plane wave expansion of the fundamental solution Γ. To obtain one, we use a more concise expression for Γ than the one in (4). Namely, we use

$$\Gamma_{ij}(x,t) = \frac{1}{\rho}\left[\partial_i\partial_j\int\int\frac{\delta(t-|x|/c_L)}{4\pi|x|}dtdt + e_{pik}e_{qjk}\partial_p\partial_q\int\int\frac{\delta(t-|x|/c_T)}{4\pi|x|}dtdt\right] \tag{6}$$

where e_{ijk} is the alternating symbol. From this expression, we see that the plane wave expansion of Γ is obtained from a similar expansion for the function

$$\Lambda_{ij}(x,t;c) = \partial_i\partial_j\int\int\frac{\delta(t-|x|/c)}{4\pi|x|}dtdt,$$

where c is a positive constant.

In order to expand Λ_{ij} into plane waves, we start from the Fourier transform of Λ with respect to space and time:

$$\frac{\xi_i\xi_j}{\omega^2(|\xi|^2 - \omega^2/c^2)} \tag{7}$$

where ξ_i and ω are the spatial and time Fourier parameters. In the inverse transform of (7) we use the well-known limiting absorption principle which states that a causal (anti-causal) Fourier inverse transform (see (8) for the definition) is obtained as one takes the ω integral on the real axis as the limit from the $\text{Im}\,\omega > 0$ ($\text{Im}\,\omega < 0$) side in the complex plane. Therefore the integral

$$\lim_{\text{Im}\,\omega \to \pm 0}\frac{1}{(2\pi)^4}\int\int\int\int\frac{\xi_i\xi_j e^{i\xi\cdot x - i\omega t}}{\omega^2(|\xi|^2 - \omega^2/c^2)}d\xi_1 d\xi_2 d\xi_3 d\omega \tag{8}$$

gives $\Lambda_{ij}(x,t;c)$ if one takes the upper limit in (8) while the same integral will be equal to

$$\Lambda'_{ij}(x,t;c) = \partial_i\partial_j\int\int\frac{\delta(t+|x|/c)}{4\pi|x|}dtdt$$

if the other limit is taken.

We now rewrite the integral in (8) into the following form:

$$\lim_{\text{Im}\,\omega \to \pm 0}\frac{1}{(2\pi)^4}\int\int\int\int\frac{\xi_i\xi_j e^{i\xi\cdot x - i\omega t}}{\omega^2(|\xi|^2 - \omega^2/c^2)}d\xi_1 d\xi_2 d\xi_3 d\omega$$

$$= \mp\frac{t}{8\pi}\partial_i\partial_j\frac{1}{|x|} + \frac{1}{(2\pi)^4}\lim_{\text{Im}\,\omega \to \pm 0}\oint\int\int\int\frac{\xi_i\xi_j e^{i\xi\cdot x - i\omega t}}{\omega^2(|\xi|^2 - \omega^2/c^2)}d\xi_1 d\xi_2 d\xi_3 d\omega, \tag{9}$$

where the sign of integration with a superimposed $=$ indicates that the integral is taken in the sense of the finite part. We next assume $x_3 > 0$ to evaluate the 2nd term on the RHS of (9), denoted by I, in the following form:

$$I = \frac{1}{2(2\pi)^3} \lim_{\mathrm{Im}\,\omega \to \pm 0} \fint \int \int \frac{\xi_i \xi_j e^{i(\xi_1 x_1 + \xi_2 x_2) - \sqrt{\xi_1^2 + \xi_2^2 - \omega^2/c^2}\, x_3 - i\omega t}}{\omega^2 \sqrt{\xi_1^2 + \xi_2^2 - \omega^2/c^2}} d\xi_1 d\xi_2 d\omega$$

where we now have

$$\xi_3 = i\sqrt{\xi_1^2 + \xi_2^2 - \omega^2/c^2}.$$

Using the change of variables given by

$$\xi_1 = R\cos\phi, \quad \xi_2 = R\sin\phi,$$

we have

$$I = \frac{1}{2(2\pi)^3} \fint \int_0^\infty \int_0^{2\pi} \lim_{\mathrm{Im}\,\omega \to \pm 0} \frac{\xi_i \xi_j e^{i(\xi_1 x_1 + \xi_2 x_2) - \sqrt{R^2 - \omega^2/c^2}\, x_3 - i\omega t}}{\omega^2 \sqrt{R^2 - \omega^2/c^2}} R\, dR\, d\phi\, d\omega. \tag{10}$$

Splitting the domain of the R integration into subdomains $|R| > |\omega|/c$ and $|R| < |\omega|/c$ and using some changes of the variables we obtain

$$\lim_{\mathrm{Im}\,\omega \to \pm 0} \frac{1}{(2\pi)^4} \int \int \int \int \frac{\xi_i \xi_j e^{i\xi \cdot x - i\omega t}}{\omega^2 (|\xi|^2 - \omega^2/c^2)} d\xi_1 d\xi_2 d\xi_3 d\omega$$

$$= \mp \frac{t}{8\pi} \partial_i \partial_j \frac{1}{|x|} \mp \frac{\partial_t}{2(2\pi)^2 c^3} \int_{S_k \cap \{k_3 \gtrless 0\}} k_i k_j \delta(t - x_l k_l/c) dS_k$$

$$+ \frac{1}{2(2\pi)^3 c^3} \fint \int_1^\infty \int_0^{2\pi} \frac{|\omega|\, \eta_i \eta_j e^{i\frac{\omega}{c}(\eta_1 x_1 + \eta_2 x_2) - \frac{|\omega|}{c}\sqrt{\rho^2 - 1}\, x_3 - i\omega t}}{\sqrt{\rho^2 - 1}} \rho\, d\rho\, d\phi\, d\omega \tag{11}$$

where k is a unit vector and S_k is the unit sphere in $\mathbb{R}^3$. Since the last integral on the RHS is common to both approaches of ω in the complex plane, we take the difference between these limits in (11) to have

$$\Lambda_{ij}(x, t; c) - \Lambda'_{ij}(x, t; c) = -\frac{t}{4\pi} \partial_i \partial_j \frac{1}{|x|} - \frac{\partial_t}{8\pi^2 c^3} \int_{S_k} k_i k_j \delta(t - x \cdot k/c) dS_k. \tag{12}$$

This result holds true for negative x_3 also. Substituting (12) into (6) we obtain the plane wave expansion for the fundamental solution given by

$$\Gamma_{ij}(x, t) - \Gamma'_{ij}(x, t) = -\frac{\partial_t}{8\pi^2} \int_{S_k} \left[\frac{k_i k_j}{\rho c_L^3} \delta(t - x \cdot k/c_L) + \frac{k_p k_q e_{pik} e_{qjk}}{\rho c_T^3} \delta(t - x \cdot k/c_T) \right] dS_k. \tag{13}$$

In this expression the function Γ' stands for the 'ghost', or the anti-causal fundamental solution given by

$$\Gamma'_{ij}(x, t) = \frac{1}{\rho} \left(\Lambda'_{ij}(x, t; c_L) + e_{pik} e_{qjk} \Lambda'_{pq}(x, t; c_T) \right).$$

This function satisfies $\Gamma'(\cdot, t) = 0$ for $t > 0$, or, is 'anti-causal'.

Eq.(13) gives the plane wave expansion for Γ. One also obtains the plane wave expansion for the double layer kernel T as one substitutes (13) into (5).

Notice that the non-integral term (the first term on the RHS) in (12) vanishes as one substitutes (12) into (13). In other words, both P and S wave components in (13) (the integrals of the 1st and 2nd terms in the integrand, respectively) include non-causal terms in addition to causal Λ_{ij} and anti-causal Λ'_{ij} and these non-causal terms cancel with each other. This means that the P (S) wave component in (13) does not vanish before the arrival of P (S) wave, even after the ghost vanishes. One therefore has to evaluate both P and S wave components in (13) together even in situations where the physics tells that only the P wave should be present.

2.3 Evaluation of potentials with the plane wave expansion

We now describe a PWTD algorithm to evaluate potentials in the time domain elastodynamics using the expansion in (13).

Let S_s and S_o be disjoint spherical domains with radius of R centred at s and o, respectively. The distance between s and o, or $|o - s|$, will be denoted by R_c ($> 2R$). Also, assume that S_s includes a part of S denoted by S_*. We are now interested in evaluating the single and double layer potentials produced by densities t and u on $S_* \times (0, t]$ and observed at (x, t) ($x \in S_o$, $t \in (0, \infty)$).

Eq.(13) shows that the plane wave expansion for the fundamental solution includes a non-physical ghost. In utilising this expansion we have to develop an approach which guarantees that the ghost does not pollute the solution. In order to obtain such an approach, we follow the developments of Ergin et al. [5] to write the density functions u and t as sums of functions u^z and t^z ($z = 1, 2, \ldots$), which have supports in the finite interval $(T_1^z, T_2^z]$:

$$u = \sum_z u^z, \quad t = \sum_z t^z.$$

Since we are interested in applying the plane wave expansion in the evaluation of the the part of integrals in the discretised integral equation in (3) which represent the effect from the past, we may assume that the integrals including u^z and t^z are evaluated only for $t > T_2^z$. As one sees from Fig. 1 the signal from $S_s \times (T_1^z, T_2^z]$ reaches S_o after $t = T_2^z$ if

$$R_c - 2R \geq c_L(T_2^z - T_1^z) \tag{14}$$

holds. One also sees that the ghost will never pollute the solution if the condition in (14) is satisfied since the ghost will vanish before the arrival of the signal.
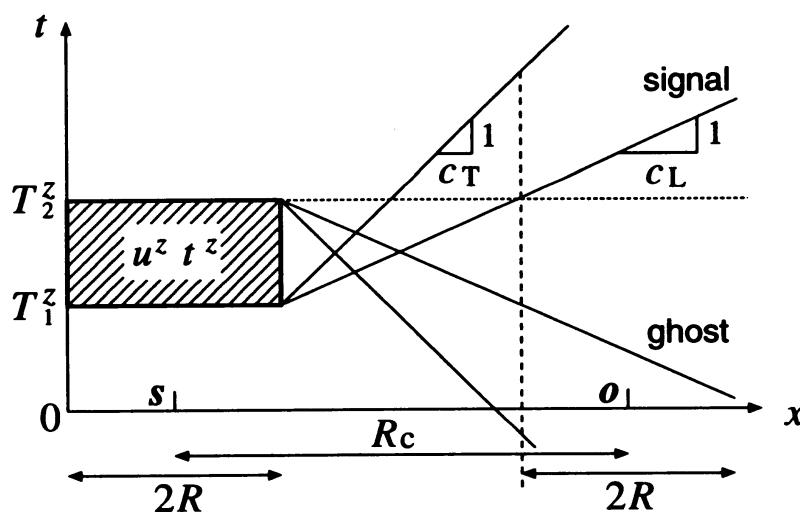

Fig. 1 Signal and ghost

If the condition in (14) is satisfied, one can evaluate potential functions in elastodynamics for (x, t) ($x \in S_o, t > T_2^z$) and known densities t^z and u^z in $(S_* \times (T_1^z, T_2^z])$ via

$$\int_{S_*} \left(T_{ij}(x, y, t) * u_j^z(y, t) - \Gamma_{ij}(x - y, t) * t_j^z(y, t) \right) dS_y$$

$$= -\frac{\partial_t}{8\pi^2} \int_{S_k} [k_i \delta(t - (x - s) \cdot k/c_L) * O^z(s, t, k) + e_{pik}k_p\delta(t - (x - s) \cdot k/c_T) * O_k^z(s, t, k)] dS_k \tag{15}$$

where the functions O^z and O_k^z ($k = 1, 2, 3$), called outgoing rays, are defined by

$$O^z(s, t, k)$$

$$= \int_{S_*} \left(\frac{C_{jlnm}n_l k_m k_n}{\rho c_L^4} \dot{u}_j^z(y, t - (s - y) \cdot k/c_L) - \frac{k_j}{\rho c_L^3} t_j^z(y, t - (s - y) \cdot k/c_L) \right) dS_y, \tag{16a}$$

$$\mathcal{O}_k^z(s,t,k)$$

$$= \int_{S_*} \left(\frac{C_{jlnm}n_l e_{qmk}k_q k_n}{\rho c_T^4} \dot{u}_j^z(y, t - (s - y) \cdot k/c_T) - \frac{e_{qjk}k_q}{\rho c_T^3} t_j^z(y, t - (s - y) \cdot k/c_T) \right) dS_y. \quad (16b)$$

The outgoing rays are considered to be the time domain counterparts of the multipole moments in the Fast Multipole Method (FMM). Notice that the elastodynamic potential functions are now expressed in terms of 4 components (one from $\mathcal{O}$ and three from $\mathcal{O}_k$) of the outgoing rays. The same property has been observed in elastostatics as well as in elastodynamics in frequency domain [2].

For (x, t) $(x \in S_o, t > T_2^z)$ one can further rewrite (15) into

$$\int_{S_*} \left(T_{ij}(x, y, t) * u_j^z(y, t) - \Gamma_{ij}(x - y, t) * t_j^z(y, t) \right) dS_y$$

$$= -\frac{1}{8\pi^2} \int_{S_k} [k_i \delta(t - (x - o) \cdot k/c_L) * \mathcal{I}^z(o, t, k) + e_{pik}k_p \delta(t - (x - o) \cdot k/c_T) * \mathcal{I}_k^z(o, t, k)] dS_k \quad (17)$$

where the functions $\mathcal{I}^z$ and $\mathcal{I}_k^z$ ($k = 1, 2, 3$), called the incoming rays, are defined by

$$\mathcal{I}^z(o, t, k) \;=\; \mathcal{T}(o - s, t, k; c_L) * \mathcal{O}^z(s, t, k), \quad (18a)$$

$$\mathcal{I}_k^z(o, t, k) \;=\; \mathcal{T}(o - s, t, k; c_T) * \mathcal{O}_k^z(s, t, k). \quad (18b)$$

and

$$\mathcal{T}(o - s, t, k; c) = \partial_t \delta(t - (o - s) \cdot k/c).$$

The incoming rays are conceptually similar to the coefficients of the local expansion in FMM. Also, the expansion in (17) and the relations in (18) are considered to be the time domain counterparts of the local expansion and the M2L relation in the original FMM.

Finally one sums up the contributions from the zth time intervals given by (17) to compute the elastic potential due to u and t defined in $S_* \times (0, t]$ and observed at $x \in S_o, t > T_2^z$ by

$$\int_{S_*} \left(T_{ij}(x, y, t) * u_j(y, t) - \Gamma_{ij}(x - y, t) * t_j(y, t) \right) dS_y = -\sum_{v=1}^{z} \frac{1}{8\pi^2}$$

$$\times \int_{S_k} [k_i \delta(t - (x - o) \cdot k/c_L) * \mathcal{I}^v(o, t, k) + e_{pik}k_p \delta(t - (x - o) \cdot k/c_T) * \mathcal{I}_k^v(o, t, k)] dS_k. \quad (19)$$

3 PWTD Algorithm for elastodynamics

In this section we shall describe a multi-level PWTD algorithm for elastodynamics in 3D using an oct-tree structure of the boundary elements and the plane wave expansion of the potentials. We shall also discuss the complexity of the algorithm.

3.1 Computation of the outgoing rays

We now describe how we evaluate the outgoing rays in (16) using the notation $\varphi(t)$ for either of the density functions u or t.

We first discuss how we partition φ into the sum of φ^z which is nonzero only in $(T_1^z, T_2^z]$. We assume that φ is very smooth, or is band limited by ω_{max}. The time increment Δt is then chosen as $\Delta t = \pi/\omega_f$ with $\omega_f = \chi_1 \omega_{max}$, where χ_1 (> 1) stands for the over sampling ratio. As Ergin et al. suggest [5], we interpolate φ using an approximately time and band limited base function $\psi(t)$ as

$$\varphi(t) \simeq \sum_\alpha \varphi(\alpha \Delta t)\psi(t - \alpha \Delta t) \quad (20)$$

and group consecutive M terms together to define

$$\varphi^z(t) = \sum_{\alpha=(z-1)M+1}^{zM} \varphi(\alpha \Delta t)\psi(t - \alpha \Delta t). \quad (21)$$

We thus split φ into a sum of approximately time and band limited functions φ^z with the help of M samples of φ. For the present purpose, Ergin et al. [5] suggest to use the following function for ψ:

$$\psi(t) = \frac{\omega_0}{\omega_f} \frac{\sin(\omega_0 t)}{\omega_0 t} \frac{\sin\left(\Omega p_t \Delta t \sqrt{(t/p_t \Delta t)^2 - 1}\right)}{\sinh\left(\Omega p_t \Delta t\right) \sqrt{(t/p_t \Delta t)^2 - 1}} \tag{22}$$

where $\omega_0 = \omega_{max}(\chi_1 + 1)/2$, $\Omega = \omega_{max}(\chi_1 - 1)/2$, and $p_t > 0$ is an integer. In (22) we interpret $\sqrt{(t/p_t \Delta t)^2 - 1} = i\sqrt{1 - (t/p_t \Delta t)^2}$ when $t < p_t \Delta t$. It is seen that ψ is band limited by ω_f and almost vanishes for $|t| > p_t \Delta t$ [5]. Hence, φ^z is certainly band limited and approximately time limited. Since one has

$$T_1^z = ((z-1)M + 1 - p_t)\Delta t, \quad T_2^z = (zM + p_t)\Delta t \tag{23}$$

from (21), one sees that the condition in (14) is satisfied if one sets M so that

$$M \leq \frac{R_c - 2R}{c_L \Delta t} - 2p_t + 1 \tag{24}$$

holds. The parameter p_t is selected appropriately considering the accuracy and efficiency of the analysis. One may generally say that a large p_t will be desirable from the point of view of the accuracy of (20), while taking p_t too large will make M in (24) small or even negative, thus making the analysis inefficient.

With φ^z thus constructed, one may use a numerical quadrature on boundary elements and the definition in (16) to compute the outgoing rays produced by densities on S_*. The time derivative for u^z included in (16) may easily be obtained with the help of FFT.

In the sequel, we shall call the time interval $((z-1)M\Delta t, zM\Delta t]$ $(z = 1, 2, \ldots)$ the zth time interval. Notice that this time interval is included in $(T_1^z, T_2^z]$ as one can see in Fig. 2.
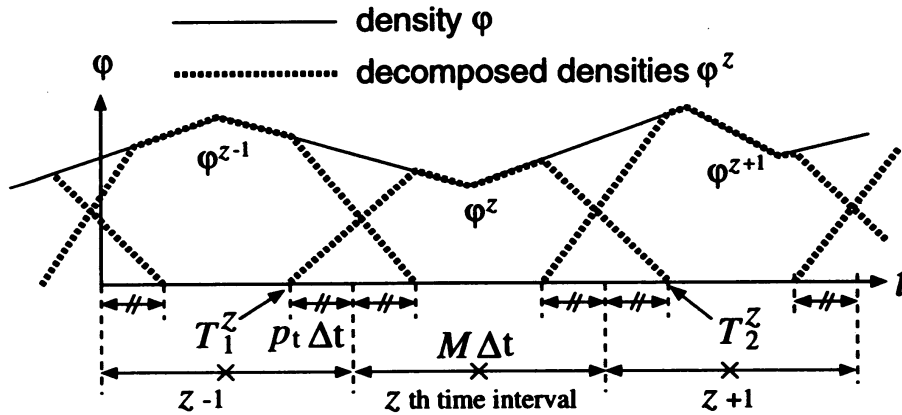

Fig. 2 Decomposition of a density φ to φ^z

3.2 Discretisation of integrals on the unit sphere

In the numerical analysis the integral on the unit sphere S_k in (17) has to be evaluated with a certain numerical integration. It is obviously necessary to select an appropriate set of ks as the integration points. A reasonable choice is obtained as one considers the process of computing the outgoing and incoming rays.

We remember that the densities $u^z(t)$ and $t^z(t)$ are band-limited to ω_f, so that the wavenumber of the densities is estimated to be ω_f/c at the largest, where c is the velocity of the relevant wave. Therefore the outgoing rays from sources distributed in the source sphere S_s, which has a radius of R, will be represented by spherical harmonics of the order of

$$K = \frac{2R\omega_f \chi_2'}{c_T}. \tag{25}$$

(cf $c_L > c_T$). The integral on the RHS of (19) is now approximated as

$$\int_{S_*} \left(T_{ij}(x, y, t) * u_j^z(y, t) - \Gamma_{ij}(x - y, t) * t_j^z(y, t)\right) dS_y$$

$$\simeq \quad -\frac{1}{8\pi^2} \sum_{p=0}^{K} \sum_{q=-K}^{K} w_{pq} \left[(k_{pq})_i \delta(t - (x - o) \cdot k_{pq}/c_L) * T(o - s, t, k_{pq}; c_L) * \mathcal{O}^z(s, t, k_{pq}) \right.$$

$$\left. + e_{jik}(k_{pq})_j \delta(t - (x - o) \cdot k_{pq}/c_T) * T(o - s, t, k_{pq}; c_T) * \mathcal{O}_k^z(s, t, k_{pq}) \right] \tag{26}$$

$$= \quad -\frac{1}{8\pi^2} \sum_{p=0}^{K} \sum_{q=-K}^{K} w_{pq} \left[(k_{pq})_i \delta(t - (x - o) \cdot k_{pq}/c_L) * \mathcal{I}^z(o, t, k_{pq}) \right.$$

$$\left. + e_{jik}(k_{pq})_j \delta(t - (x - o) \cdot k_{pq}/c_T) * \mathcal{I}_k^z(s, t, k_{pq}) \right] \tag{27}$$

where k_{pq}, w_{pq}, θ_p and ϕ_q $(p = 0, \ldots, K, q = -K, \ldots, K)$ are defined by

$$k_{pq} = \sin\theta_p \cos\phi_q i_1 + \sin\theta_p \sin\phi_q i_2 + \cos\theta_p i_3, \tag{28a}$$

$$w_{pq} = \frac{4\pi \sin^2\theta_p}{(2K+1)\left[(K+1)P_K(\cos\theta_p)\right]^2}, \tag{28b}$$

$$\theta_p = (p+1)\text{th root of equation } P_{K+1}(\cos\theta) = 0, \tag{28c}$$

$$\phi_q = \frac{2\pi q}{2K+1} \tag{28d}$$

in terms of the orthonormal base vectors i_k for the cartesian coordinate axis.

3.3 Description of the algorithm

To solve the BIE given by (3), we have to evaluate elastic potentials with known densities. In fast algorithms of the multi-level FMM type to evaluate these potentials at a point x, we split the boundary into two parts: i.e. the part $S_f^{(l)}(x)$ which is far from x and $S_n^{(l)}(x) = S \setminus S_f^{(l)}(x)$ which is close to x. The contributions to the potentials from $S_f^{(l)}(x)$ is computed with the help of the plane wave expansion, while the evaluation of the contributions from $S_n^{(l)}(x)$ is passed to $l + 1$th level. At the deepest level (largest l), we compute the contributions from $S_n^{(l)}(x)$ directly using the conventional methods.

To describe this algorithm more precisely, we have to define what we mean by the words 'far' and 'level'. We first discretise the boundary integral equation (3) using boundary elements having N_s spatial degrees of freedom and N_t time intervals of the length Δt. For definiteness, we assume the boundary elements to be piecewise constant and the time base functions to be piecewise linear, although these assumptions are not essential.

We next construct the oct-tree structure of boundary elements in the following manner. We first take a cube which includes the domain D. This cube is called the cell of the level 0. This cube is subdivided into 8 equal sub-cubes, of which those containing boundary elements are called cells of the level 1. We repeat this subdivision until the cell contains less than a fixed number (denoted by N_{cell}) of boundary elements. A cell without children is called a leaf, and the level number of the deepest cell is denoted by l_{max}.

We say two cells C and C' of the level l to be close if

$$|C_i - C_i'| < (\beta + 1)L^{(l)} \quad i = 1, 2, 3 \tag{29}$$

holds, where C_i and C_i' are the coordinates of the centroids of C and C', β is a natural number and $L^{(l)}$ is the edge length of the level l cell. With this definition, the set $S_n^{(l)}(x)$ is defined to be the union of level l cells C' which is close to C if $x \in C$. The cells C' of the level l which are not close to C are said to be far from C. In Fig.3 we have indicated cells close to the cell C when β is equal to 1. In the rest of this paper we shall assume that $\beta = 1$.

In the evaluation of elastic potentials at a point x in a level l cell C, we shall use the plane wave expansion when we compute the effects from boundary elements included in a level l cell C' which is far from C. The contributions from far cells are evaluated in the form of the incoming rays associated with C.

To compute contributions from cells far from C, we have to determine, for each level l, numbers $R^{(l)}$, $R_c^{(l)}$, $T_1^{z^{(l)}}$, $T_2^{z^{(l)}}$ and $M^{(l)}$ which satisfy (14) and (24), where the superposed (l) indicates that the associated quantity is for level l cells. It is considered natural to set

$$R^{(l)} = \frac{\sqrt{3}L^{(l)}}{2}, \quad R_c^{(l)} = 2L^{(l)},$$

except in (14), whose LHS can be put equal to $\beta L^{(l)}$ $(= L^{(l)})$, since it is sufficient to set the LHS of (14) as the minimum distance between S_o and S_s. Accordingly, one puts $M^{(l)}$, $T_1^{z^{(l)}}$ and $T_2^{z^{(l)}}$ to be

$$M^{(l_{max})} = \frac{L^{(l_{max})}}{c_L \Delta t} - 2p_t + 1,$$
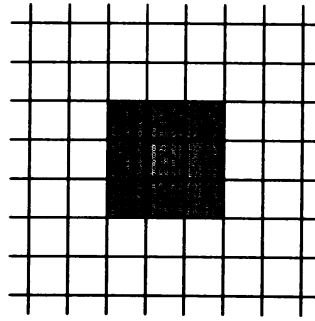
$\beta = 1$

Fig. 3 Near cells for a cell C

$$
\begin{aligned}
M^{(l)} &= 2M^{(l+1)}, \quad (l < l_{max}) \\
T_1^{z^{(l)}} &= ((z^{(l)} - 1)M^{(l)} + 1 - p_t)\Delta t, \\
T_2^{z^{(l)}} &= (z^{(l)}M^{(l)} + p_t)\Delta t
\end{aligned}
$$

where the constant p_t is taken independent of the level. Also we use (25) to have

$$
K^{(l)} = \frac{2R^{(l)}\omega_f \chi_2'}{c_T} \left(= \frac{\sqrt{3}L^{(l)}\omega_f \chi_2'}{c_T} \right), \tag{30}
$$

which implies the following relation:

$$
K^{(l)} = 2K^{(l+1)}.
$$

Also, from (28) we have

$$
k_{pq}^{(l)} = \sin\theta_p^{(l)} \cos\phi_q^{(l)} i_1 + \sin\theta_p^{(l)} \sin\phi_q^{(l)} i_2 + \cos\theta_p^{(l)} i_3, \tag{31a}
$$

$$
w_{pq}^{(l)} = \frac{4\pi \sin^2\theta_p^{(l)}}{(2K^{(l)} + 1)\left[(K^{(l)} + 1)P_{K^{(l)}}(\cos\theta_p^{(l)})\right]^2}, \tag{31b}
$$

$$
\theta_p^{(l)} = (p+1) \text{ th root of equation } P_{K^{(l)}+1}(\cos\theta) = 0, \tag{31c}
$$

$$
\phi_q^{(l)} = \frac{2\pi q}{2K^{(l)} + 1}. \tag{31d}
$$

We now describe the algorithm to solve (3) using the plane wave expansion and an iterative solver.

1. Initial guess

   Let the current time be $t_\alpha = \alpha\Delta t$ ($\alpha = 1, 2, \ldots, N_t$) and all the boundary displacements and tractions in the past, i.e. $u(\cdot, t_{\alpha'})$ and $t(\cdot, t_{\alpha'})$ for $t_{\alpha'}$ ($\alpha' = 1, \ldots, \alpha - 1$), are known.

   We then provide initial guesses to the unknown parts of $u(\cdot, t_\alpha)$ and $t(\cdot, t_\alpha)$ arbitrarily. Giving the values for the same quantities at $t_{\alpha-1}$ would be a reasonable choice.

2. Evaluation of potentials due to sources on $S \times (0, t_\alpha]$

   As the density functions on $S \times (0, t_\alpha]$ are given, the potentials in (3) for each collocation point x due to sources on $S \times (0, t_\alpha]$ are divided into contributions from the near part $S_n^{(l)}(x) \times (0, t_\alpha]$ and far part $S_f^{(l)}(x) \times (0, t_\alpha]$.

2a. Contributions from the near part $S_n^{(l)}(x) \times (0, t_\alpha]$

   For each cell (denoted by C) of the level l ($l \geq 2$), use the conventional direct integration to compute contributions to the elastic potentials at the collocation points (x, t_α) ($x \in C$) from densities $u(\cdot, t_{\alpha'})$ and $t(\cdot, t_{\alpha'})$ ($\alpha' = 1, \ldots, \alpha$) distributed in a neighbouring cell C' of the level l (including C itself) if either C or C' is a leaf.

2b. Contributions from the far part $S_f^{(l)}(x) \times (0, t_\alpha]$

Let l be the level of the leaf containing x. We note the following: for a level l cell, the time t_α belongs to the $z_\alpha^{(l)}$th time interval, where $z_\alpha^{(l)} = \lfloor \alpha/M^{(l)} \rfloor$ and $\lfloor \cdot \rfloor$ stands for the 'floor' operation. At t_α the outgoing rays $\mathcal{O}^{z^{(l)}}$ (in the rest of this paper we shall use a collective notation $\mathcal{O}^{z^{(l)}}$ for $(\mathcal{O}^{z^{(l)}}, \mathcal{O}_t^{z^{(l)}})$) and the incoming rays $\mathcal{I}^{z^{(l)}}$ corresponding to $z^{(l)} = 1, 2, \ldots, z_\alpha^{(l)} - 1$ are all known (see the procedure in 4b below). The incoming rays $\mathcal{I}^{z^{(l)}}$ determine the layer potentials due to densities $u^{z^{(l)}}$ and $t^{z^{(l)}}$ distributed in $S_f^{(l)}(x) \times (T_1^{z^{(l)}}, T_2^{z^{(l)}}]$ via (27), which we have had already computed in step 4b. Namely, at the collocation point (x, t_α) the layer potentials due to densities $\sum_{z^{(l)}=1}^{z_\alpha^{(l)}-1} u^{z^{(l)}}$ and $\sum_{z^{(l)}=1}^{z_\alpha^{(l)}-1} t^{z^{(l)}}$ on $S_* \times (0, T_2^{z_\alpha^{(l)}-1}]$ have been computed and stored. One just recalls the values thus stored. We note that the potentials due to densities distributed on $S_f^{(l)}(x) \times (T_2^{z_\alpha^{(l)}-1}, t_\alpha]$ will not reach collocation points (x, t_α) before $t = T_2^{z_\alpha^{(l)}}$, and do not have to be taken into consideration. We have thus evaluated potentials due to densities in $S_f^{(l)}(x) \times (0, t_\alpha]$.

3. Determination of the current unknowns

We update the unknowns at $t = t_\alpha$ following the procedures of the iterative solver used and return to step 1 if the discretised version of the BIE in (3) is not satisfied to within an allowable error. Otherwise the assumed values for the unknowns at $t = t_\alpha$ are adopted as the solution at t_α. If $\alpha < N_t$ we go to step 4. Otherwise we terminate the analysis.

4. Computation of outgoing rays and incoming rays

Compute the outgoing and incoming rays for $z_\alpha^{(l)}$ in the following manner:

4a. Computataion of the outgoing rays (upward)

Starting from leaves up to level 2 cells we compute the outgoing rays $\mathcal{O}^{z_\alpha^{(l)}}$ at the centroid of the cell for the $z_\alpha^{(l)}$th time interval if and only if the current time step number α is a multiple of $M^{(l)}$. To compute $\mathcal{O}^{z_\alpha^{(l)}}$ we use the definition in (16) if C is a leaf. For non-leaf cells we add the outgoing rays of the child cells $\mathcal{O}^{z_\alpha^{(l+1)}-1}$ and $\mathcal{O}^{z_\alpha^{(l+1)}}$ after shifting the centres of the expansion from those of the children (s') to that of C (s). Since upper cells require more directions (k) than the lower ones because of (30), we have to increase the number of directions as we go up the tree structure of cells. To cope with this requirement we use an operation called 'interpolation'. See [5] for the detail.

4b. Computation of the incoming rays (downward)

Starting from level 2 cells we compute the incoming rays for the current ($z_\alpha^{(l)}$th) time interval at the centroids of level l cells if and only if the current time step number α is a multiple of $M^{(l)}$, as in step 4a. In this process we define the incoming rays associated with a level l cell C to be the sum of the incoming rays from all the level l cells (denoted collectively by C') which are not close to C. Such C's consist of level l cells which are not close to C but whose parents are close to the parent of C (interaction list) and those whose parents are not close to the parent of C. The contributions to $\mathcal{I}^{z_\alpha^{(l)}}$ from the former (cells in the interaction list of C) are evaluated via (18), but in the frequency domain using a smoothed T (See [5]). On the other hand, the contributions from the latter C's are obtained as one shifts the incoming rays of the parent of C ($\mathcal{I}^{z_\alpha^{(l-1)}}$) from the centroid of the parent (o') to that of C (o). Notice that the number of directions k required for C is less than that possessed by the parent. Therefore one has to 'anterpolate' the incoming rays in the downward path of the algorithm [5]. When C is a leaf, one uses the incoming rays for C thus obtained ($\mathcal{I}^{z_\alpha^{(l)}}$) and (27) to compute the elastic potentials for $t > T_2^{z_\alpha^{(l)}}$ due to u and t in the past distributed in far cells. The computation is carried out in the 'cast forward' manner with respect to time, and stored. The results will be recalled in step 2b later.

5. Update

Update α by $\alpha + 1$ and go to step 1.

.4 Complexity of the algorithm

/e consider a series of problems with increasing domain size solved with the same accuracy (i.e. the number of nodes ?r wave length remains constant). Ergin et al. [5] estimated that the complexity of their PWTD algorithm for the ave equation in 3D applied to the series of problems of this type is $O(N_s \log^2 N_s N_t)$. Using the same argument as Ergin et al., one shows that the complexity of the part of the present algorithm using the plane wave expansion is

identical with that of Ergin et al. One also shows that the direct computation part of the elastodynamic algorithm scales as $O(N_s N_t)$ in spite of the time integration included in the potential representation of the solution. This is because the elastodynamic fundamental solution in 3D vanishes after the time required for S waves generated at the collocation point x to sweep out the part of the boundary where the contribution to the potentials at x is evaluated directly. One therefore concludes that the overall complexity of the proposed approach is $O(N_s \log^2 N_s N_t)$ if one follows closely the approach proposed by Ergin et al.

Ergin et al., however, assumes that they use a fast method of evaluating the Legendre transform [6] in the interpolation and anterpolation to establish their complexity estimate. Since our implementation uses the standard (sometimes called 'semi-fast') algorithm [6] for this purpose, however, our algorithm cannot be faster than $O(N_s^{3/2} N_t)$. In problems of the size considered in this paper, it may not be obvious if the use of 'fast' methods for the Legendre transform actually improves the performance of the algorithm or not.

4 Numerical analysis

4.1 Details of the present implementation

In the following examples we use GMRES without preconditioning as the iterative solver to obtain the solution of discretised version of (3) in both fast and conventional BIEM. As the initial guess, we use zero for the first time step, and the solutions at the previous time step for the rest of analysis

As has been seen, our implementation requires the following parameters: N_{cell}: maximum number of boundary elements in a leaf cell (see 3.3), p_t: parameters related to the interpolation functions with respect to time(see (22)), χ_1: over sampling rate, Δt: time increment which is related to the maximum frequency of the field quantities ω_{max} by $\omega_{max} = \pi/(\chi_1 \Delta t)$ and χ_2': a parameter related to the number of directions k (see (25)). The following choices of the parameters are used in the examples given below: $\chi_1 = 3.0$, $\chi_2' = 0.2$ and $p_t = 3$. This choice for χ_1 means that one uses 6 time nodes per the shortest of the expected periods. Also, we have used an appropriate non-dimensionalisation to set $c_L = 1$, $c_T = 1/\sqrt{2}$ and $\rho = 1$. This means that the Poisson's ration is equal to 0.

In the computation we have used Fujitsu VPP800/63 with 7GB of the main memory. The code is not parallelised.

4.2 Numerical example

We consider as the domain D a parallelepiped having the line connecting $(0,0,0)$ and (X,Y,Z) as the space diagonal. In the initial boundary value problem considered, the initial displacement and velocity are assumed to vanish. As the boundary condition we prescribe the traction computed from the following field:

$$u(x,t) = d \left[1 - \text{Cos} \frac{2\pi}{\Lambda} \left(t - \frac{d \cdot x}{c_L} \right) \right],$$ (32)

where d is a unit vector and the function Cos is defined by

$$\text{Cos}\, x = \begin{cases} \cos x & 0 \leq x \leq 2\pi \\ 1 & x < 0, \ x > 2\pi \end{cases}$$ (33)

The function u obviously represents a plane P wave propagating into the direction d. The solution to the problem under consideration is obviously u itself. We set $d = (0,0,1)$, $\Lambda = 0.5$, $Z = 0.80$ and $N_t = 200$. For the parameters X and Y we consider the 10 cases listed in Table 1 . This table also shows N_s. See Fig. 4 (this figure shows the case 10 in Table 1) for an example of the boundary discretisation. Other parameters are set as $\Delta t = 0.01$ and $N_{cell} = 150$. The depth of the oct-tree l_{max} is equal to 2 in case 2, 3 in cases 2–9, and 4 in case 10. We note that the choice $\chi_2' = 0.2$ yields that the number $K^{(2)}$ to be 24 in cases 1–9 and 56 in case 10. The number of directions in level 2 cells is then given by $(K^{(2)} + 1)(2K^{(2)} + 1)$.

Table 1 X, Y, Z and N_s

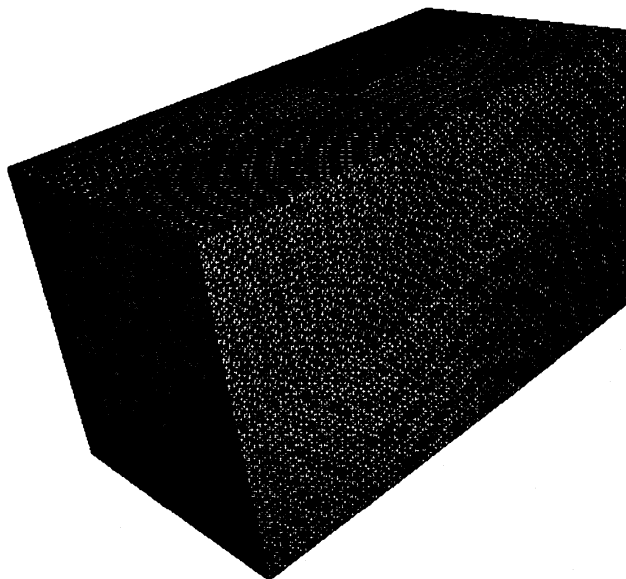| case	1	2	3	4	5	6	7	8	9	10
X	0.12	0.12	0.16	0.16	0.20	0.24	0.20	0.40	0.80	1.40
Y	0.12	0.16	0.16	0.20	0.20	0.24	0.68	0.68	0.68	0.68
Z	0.80	0.80	0.80	0.80	0.80	0.80	0.80	0.80	0.80	0.80
N_s	2,064	2,432	2,816	3,200	3,600	4,416	8,400	11,360	17,280	26,160

Fig. 4 Boundary element discretisation used in case 10 (78,480 DOF)

Fig. 5 shows the CPU time(sec.) vs the number of unknowns N_s. This figure shows that the present method is capable of carrying out elastodynamic analysis in time domain more efficiently than the conventional method in all the examples considered. The fluctuation of the CPU time for small N_s seems to be due to the condition of the computer, which is shared by many users.

Because of the restriction of the memory it was not possible to solve cases 5–10 with the conventional BIEM. If CPU time is not important, however, one may use the conventional method in larger problems by not storing all the integration results, but by recalculating them when needed. In this way we could solve all the cases with the conventional approach using a desktop computer (Alpha21264 (600[MHz]), 2[GB] of memory), and could compare the results of the proposed and conventional approaches in all cases. It was found that the maximum error of the boundary displacements (relative to the maximum boundary displacement (=2)) was about 3% in both proposed and conventional methods.

We finally remark that the following url includes animations of other examples solved with the proposed method.

http://geehost.gee.kyoto-u.ac.jp/~ttaka/eabe.html

5 Conclusion

In this paper we could successfully extend the PWTD algorithm proposed for the wave equation by Ergin et al. [5] to elastodynamics in 3D. We could also show the effectiveness of the proposed approach in simple test problems of the spatial size of $O(10^4)$.

Since the method is still in its incipient stage of developments we still need to refine the code so that it can be applied to larger problems found in engineering applications. However, the fundamentals of the approach are now established and the numerical results seem to be promising.

References

[1] Kobayashi S et al.. Wave Analysis and Boundary Element Methods. Kyoto University Press; 2000 (in Japanese).

[2] Nishimura N. Fast multipole accelerated boundary integral equation methods. accepted for publication in Applied Mechanics Reviews 2002.

[3] Takahashi T, Nishimura N, Kobayashi S. Fast boundary integral equation method for elastodynamic problems in 2D in time domain. Trans JSME 2001;A67-661:1409–16 (in Japanese).
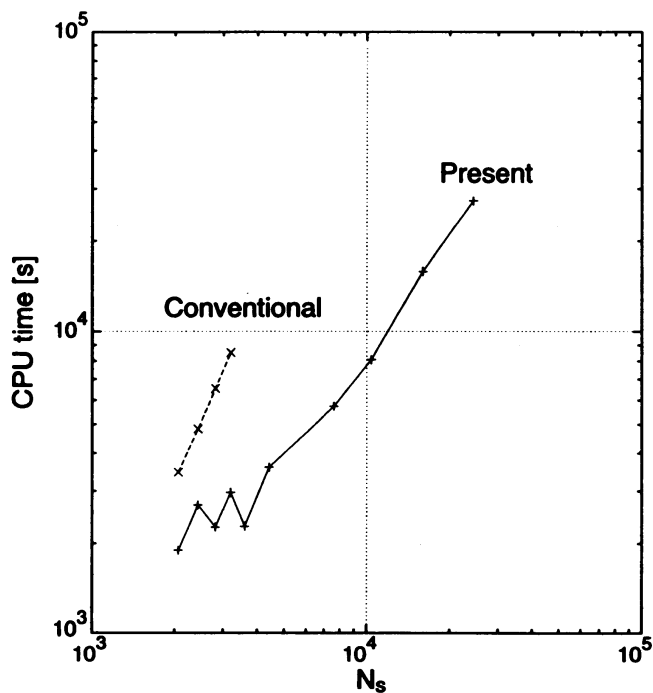
Fig. 5 Comparison of computational time

[4] Lu M, Wang J, Ergin AA, Michielssen E. Fast evaluation of two-dimensional transient wave fields. J Comput Phys 2000;158:161–85.

[5] Ergin AA, Shanker B, Michielssen E. Fast analysis of transient acoustic wave scattering from rigid bodies using the multilevel plane wave time domain algorithm. J Acoust Soc Am 2000;107:1168–78.

[6] Chien RJ, Alpert BK. A fast spherical filter with uniform resolution. J Comput Phys 1997;136:580–4.